

Geometry-Informed Transmission Strength Scaling in Barrage Relay Networks

Brent Kraczek¹ and Nicholas Woolsey²

¹DEVCOM Army Research Laboratory, Aberdeen Proving Ground, MD, USA

²Department of Electrical and Computer Engineering, University of Utah, Salt Lake City, UT, USA

Email: {brent.e.kraczek.civ@mail.mil,nicholas.woolsey@utah.edu}

Abstract—Barrage relay networks (BRNs) are a type of ad hoc wireless network with current and proposed uses in military, disaster response, industrial and vehicle-to-vehicle applications. BRNs are designed specifically to operate robustly without any information about the relative positions of other nodes on the network. The nodes in a specific connection within a BRN are determined by the formation of a controlled barrage region (CBR). There is a trade-off between reliability and node utilization or the number of nodes that are reserved for a single unicast link. In a previous paper, we investigated the suitability of BRNs for higher-density networks, which are anticipated with the explosion of network-connected devices. We showed that node utilization increases superlinearly with both node density and the distance between source and destination, calling into question the suitability of BRNs for use in high-density networks. In this paper we use a connected graph model to show that CBR formation algorithm generates a specific geometry in the limit of infinite node density. Applying this geometry to a more physically realistic random channel model (RCM) with finite node density, we propose tuning the model by scaling the transmission power of receivers. The transmit power is based on received signal strength during the sending of request to send (RTS) and clear to send (CTS) packets, used to determine the nodes used in the CBR. We show that in discrete event simulations this signal strength scaling can reduce the utilization while simultaneously improving the probability of CBR formation.

I. INTRODUCTION

The rapid influx of inexpensive wireless devices presents a need to develop network and routing protocols for the predicted dense networks of the future [1]. Moreover, there are many advantages to design such networks to be decentralized. When nodes of a network all coordinate channel uses and communicate among one another, this eliminates the need for a high power centralized node such a cell tower. In a truly decentralized network there is no single point of failure and no need for existing backbone infrastructure. Instead, decentralized networks can be deployed anywhere instantaneously. If designed correctly, bandwidth can be better utilized by transmitting shorter ranges between nodes allowing for spatial reuse of the RF channel. Given these advantages, decentralized networks are ideal for military [2]–[4], disaster response [5], [6], industrial, resource extraction, sensor network [7], [8] and, potentially, vehicle-to-vehicle applications [9]. In the literature, these types of networks are more commonly referred to as mobile ad-hoc networks (MANETs).

Nicholas Woolsey is now with Trabus Technologies in San Diego, CA, Email: {nickw@trabus.com}.

A main challenge of MANETs is the coordination of the nodes in the network, especially determining channel access and routing of messages on the network. Protocol design must balance overhead, memory constraints and variability in time when determining how much information about the network topology to store and/or transmit. *Barrage Relay Networks* (BRNs) aim to minimize overhead while allowing for successful routing and channel coordination by storing no topology information. Inspired by Ramanathan [10], who recognized that most nodes in multihop networks act as relays, not as the source or destination, BRNs [11] seek decrease latency by handling routing in the link, rather than network, layer of the network OSI model [12]. Within a TDMA scheme, every node that receives a control or data message retransmits it in the next time slot, unless some internal control stops it. Many neighboring nodes may broadcast the same message simultaneously, with differences in phase handled using a dithering algorithm [13]. As these message use the same frequency, time and code multiplexing, all node-specific information is omitted, as it would interfere with information from neighboring nodes. To limit the number of nodes utilized (or reserved) for a single link, the routing protocol forms *Controlled Barrage Regions* (CBRs), where only nodes within this region retransmit data messages of a unicast link. These CBRs are determined through counting the number of retransmissions, or *hops*, a packet makes.

BRNs were developed by researchers at TrellisWare Technologies, Inc., and are used in radios they sell. Researchers at TrellisWare, and elsewhere, have published a number of studies on how BRNs operate. Most of this research was performed assuming a *Connected Graph Model* (CGM), in which an edge between two nodes implies that they can receive transmissions from each other [11], [14]. The CGM was later extended to include connections between all nodes within a fixed transmission radius [15].¹ Further studies have investigated how to incorporate Rayleigh fading, path loss and interference [16], [17].

In a recent paper [18], we studied the effects of cooperative broadcasting on node utilization and the reliability of forming CBRs. We developed a channel model that incorporates cooperative broadcasting consistent with Rayleigh fading, which

¹The CGM employed throughout this paper is the latter type, with cut-off radius d_0 .

we called the *Random Channel Model* (RCM).² We consider the RCM to be physically representative of how transmissions would operate, absent detailed information about the physical environment, and thus prefer it to the CGM for analysis of BRNs.

In our previous work, we explored a trade-off between reliability and node utilization in BRNs. Specifically, we found that cooperative broadcasting can act as a failure mechanism in the formation of CBRs, making it necessary to increase the parameter known as *excess width* to improve reliability. This effect was found to be particularly relevant in dense networks, where the node utilization scaled superlinearly with respect to each of, the excess width, node density and the distance between a source and destination node. This motivates our current study, which modifies the BRN protocol in a manner to reduce node utilization, while maintaining reliability.

In this paper, we use the same techniques and simulation code used in our previous paper to explore a modification to the CBR formation algorithm to decrease node utilization while maintaining reliability. This paper makes two contributions. First, we show that the formation of CBRs, a type of self-organization, can be understood geometrically, and that this directly impacts node utilization. Second, we use this geometric understanding to design a new method for strategic transmit power control that can prevent messages from propagating too far on the network. This modification is consistent with BRN principle that nodes transmit no information about themselves, so that all relaying can be kept within the link layer. In our results, we find that this power scaling achieves the desired aims for utilization and reliability.

The remainder of the paper is organized as follows. In Section II, we show how, within the CGM, the geometry of a CBR can be understood in terms of concentric circles and ellipses. In Section III, we use this geometric understanding, and the differences between the CGM and RCM, to modify the CBR formation algorithm to significantly reduce node utilization while maintaining a high level of reliability. We give concluding thoughts in Section IV.

II. GEOMETRY OF A CBR

While BRNs make no explicit considerations of geometry, a consistent geometry of CBRs emerges due to how the algorithm operates, and has significant impact on the efficiency of the protocol. The study of emergent geometry in networks (not limited to communications networks) is an area of active research (see [19] and references therein). For wireless communications networks, in which any node may act as source, destination or relay, node connectivity often depends on a function related to the Euclidean distance between the nodes, with consideration given to any obstacles in the way.

²We also introduced the *Deterministic Channel Model* (DCM), which operates like the RCM, without Rayleigh fading. The results for the DCM-based studies made for the previous and the current paper are similar to the results from the RCM. For the sake of brevity, we have omitted DCM results from the current paper.

Thus, an embedding space often may be assumed, reducing the complexity of the problem.

In order to understand the geometry of the CBRs, we consider the geometry of the propagating RTS and CTS packets in the two-dimensional Euclidean plane. We define the points S and D to lie at the the *Source* and *Destination* nodes, and write the distance between any two nodes M , N , as d_{MN} . We initially assume infinite node density, ρ , and CGM connectivity between all pairs of nodes separated by a distance less than the cut-off radius d_0 . For RTS packets, each node that receives an RTS packet for the first time in TDMA frame t_i , retransmits that packet in frame t_{i+1} . A node that has already received the RTS packet will not retransmit the incoming packet. Beginning from the source, within the first frame, t_1 , all nodes N such that $d_{SN} \leq d_0$ will receive the transmission, forming a circular region of radius d_0 . These nodes are considered to be one hop from the source. Counting the first frame as $i = 1$, in any subsequent frame i , a node N receiving the transmission in that frame will lie in the annular region with $(i-1)d_0 < d_{SN} \leq id_0$. For finite node densities, the boundaries of these regions will get smaller, decrease as the density decreases, and will be only approximately circular. The geometry of return transmission of CTS packets is similar to the RTS transmission.

The geometry of the final CBR in the CGM–infinite density limit, is based on an ellipse, generated by the intersection of the circles that bound the concentric annular regions of the RTS and CTS packet propagation. As illustrated in Fig. 1a., we consider a point P , that lies on the intersection of two circles, one circle centered on the source, at point S , and the other on the destination, at point D . In this idealized geometry, the distances from S and D to P are given, respectively, by

$$\begin{aligned} d_{SP} &= i_{\text{RTS}}^P d_0, \\ d_{DP} &= i_{\text{CTS}}^P d_0, \end{aligned}$$

where i_{RTS}^P and i_{CTS}^P are positive integers, counting the number of hops from S/D to P . The CBR formation procedure selects a node N as a relay node if it satisfies the criteria that the number of hops

$$i_{\text{RTS}}^N + i_{\text{CTS}}^N - i_{SD} \leq w, \quad (1)$$

where i_{SD} is the minimum number of hops required to transmit from S to D , and w is a pre-selected, non-negative integer, called the *excess width*. One property of an ellipse is that the sum of the distances from the foci to any point on the ellipse are constant. Thus, all points P with constant $d_{SP} + d_{DP}$, lie on the same ellipse. All relay nodes that satisfy equation (1) for a given w , lie within specific regions of the network, enclosed by the intersections of the bounding circles. In addition non-relay nodes one hop away from a relay node or the source or destination are labeled as buffer nodes. In figure 1a., the ellipses are drawn for $w \in \{0, 1, 2, 3\}$. In figure 1c., the regions of relay and buffer nodes are shown in blue and pink, respectively, for the same $S - D$ pair, with $w = 0$. Figure 1d., shows this same geometry, generated by a CGM

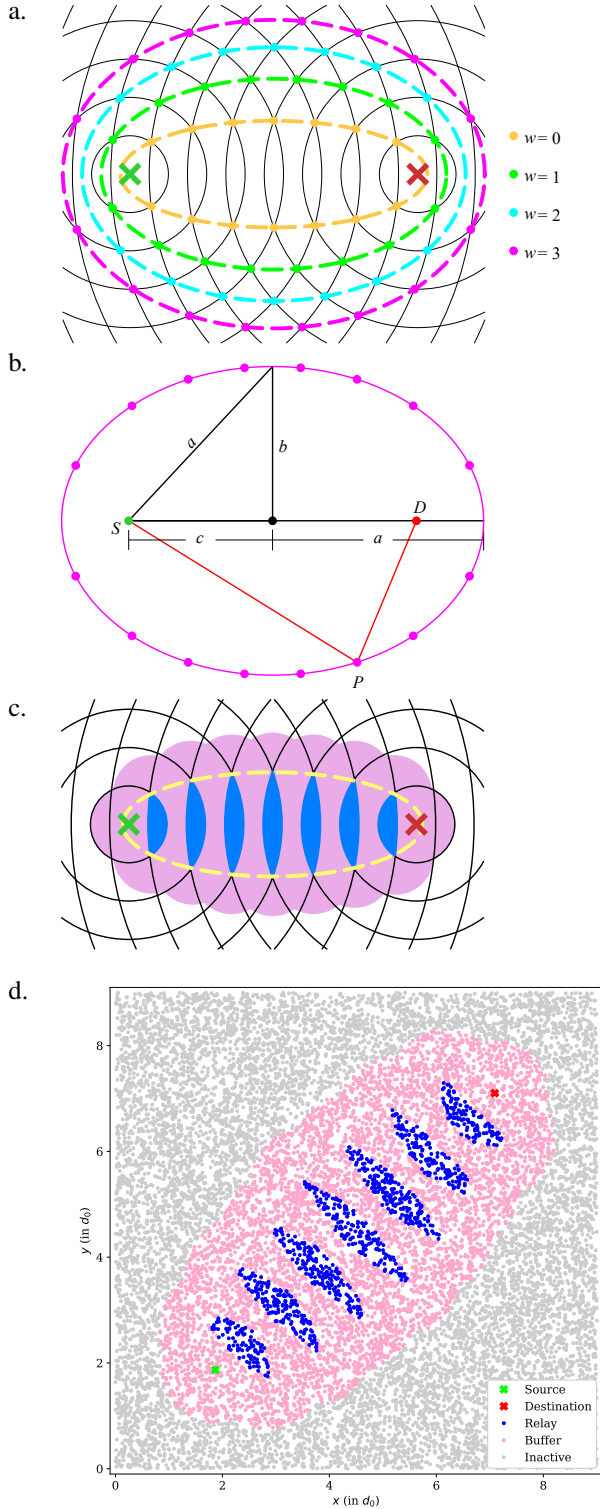


Fig. 1. How overlapping sets of concentric circles leads to an elliptical geometry. a. In the infinite density limit of the CGM, RTS and CTS packets are received by nodes within concentric annuli, with inner and outer radii of $(i-1)d_0$ and id_0 , where i is the number of hops the packet has undergone. b. A basic property of an ellipse is that all points P for which the sum of distances $d_{SP} + d_{PD}$ is a constant lie on an ellipse, with foci at S and D . c. The geometry of a CBR with $d_{SD} = 7.5$ and $w = 0$. All nodes lying in blue regions are labeled as relay nodes, while all nodes within a distance of d_0 from a relay node are labeled as buffer nodes. d. A CGM simulation of the CBR formation algorithm, producing a similar geometry, with $\rho = 200/(d_0)^2$, $d_{SD} = 7.4$ and $w = 0$.

simulation of the CBR formation algorithm, for a network with density $\rho = 200/(d_0)^2$.

In the current paper, all nodes relay and buffer nodes for a CBR are considered *utilized*. The area within the ellipse defines a geometric lower bound (LB) to the area in which all nodes are utilized. The area of an ellipse is $A = ab\pi$, where a and b are the semi-major and semi-minor axes. These are drawn in figure 1b., and form a right triangle with $c = \frac{1}{2}d_{SD}$. The sum of distances $(d_{SP} + d_{PD})$ is related to the distance d_{SD} via the ceiling function $\lceil \cdot \rceil$, w , and the semi-major axis a of the ellipse, according to

$$d_{SP} + d_{PD} = d_0 \left(\left\lceil \frac{d_{SD}}{d_0} \right\rceil + w \right), \quad (2a)$$

$$a = \frac{1}{2} (d_{SP} + d_{PD}), \quad (2b)$$

It can be shown that the area of this ellipse is given by

$$A = \pi \frac{d_0^2}{4} \left(\frac{d_{SD}}{d_0} + \delta + w \right) \cdot \left(2 \frac{d_{SD}}{d_0} (\delta + w) + (\delta + w)^2 \right)^{1/2}, \quad (3)$$

where

$$\delta = \left\lceil \frac{d_{SD}}{d_0} \right\rceil - \frac{d_{SD}}{d_0}.$$

We test these results using discrete event simulations on an ensemble of approximately 10^4 random networks, using the same methods and custom simulation code as described in our previous paper [18]. Each network is a square with side-length $25d_0$, with node densities of $\rho \in \{2, 5, 10\}/(d_0)^2$. The source-destination pairs chosen from nodes lying near the diagonal from lower left to upper right, with d_{SD} ranging from 3 to $16d_0$. Since we choose only the representative pairs closest to the diagonal, and omit repeat S-D pairs, the actual number of networks tabulated depends on ρ , and ranges from roughly 10^5 to 10^7 . The results are binned by distance d_{SD} , according to whether or not a CBR was successfully formed. We call the rate of success of domain formation the *reliability*, denoted by R . We also bin U/ρ , which is the number of nodes utilized normalized to area via the node density, and then compute the 2.5%-, 25%-, 50%-, 75%- and 97%-tile values for U/ρ .

In figure 2 we show the results of CBR formation from an ensemble of CGM discrete event simulations, for $\rho = 10/(d_0)^2$ and $w = 2$. Node utilization is represented by the percentiles plotted as a high-density box-plot, showing how the utilization distributions vary with d_{SD} . Reliability is a single curve, which, in the present case is always 1. (In general, we find the reliability of the CGM to be 1 when $\rho > 3$, regardless of w , and these calculations are consistent with the result.) We also add the geometric lower bound, *Geom. LB* for comparison. Qualitatively, the distributions of U/ρ are similar to the geometric LB: each generally increases as d_{SD} increases, but is punctuated by downward jumps, reflecting the nature of δ used in eq. (3). Because the node density in our simulations is finite, the utilization is often less than the

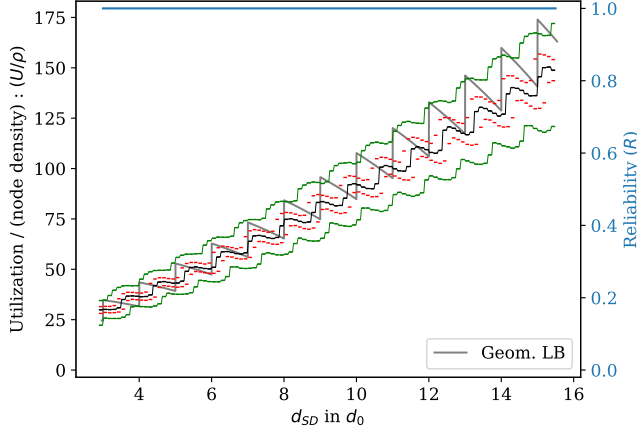


Fig. 2. Reliability and utilization results for discrete simulation of CBR formation using CGM. In this case the reliability is 1—all simulations successfully formed a CBR. The utilization per node density is plotted as a high-density box plot, showing the 95%-confidence interval (outer green envelope), the median (black center line) and the 25%- and 75%-percentiles as disjoint red line segments. The geometric LB is added as a heavy gray line for comparison, but should not be expected to match perfectly, as it assumes infinite node density.

geometric LB suggests, and the frequency of the downward jumps is a bit shorter than the expected $1 d_0$. We anticipate that in the infinite density limit, the utilization distributions would condense to their median values, which would rise above the geometric lower bound, and that this median value would have jumps at the same positions as the geometric LB.

III. GEOMETRY-GUIDED SCALING OF TRANSMISSION POWER

In this section, we use the geometric understanding developed in section II to suggest a modification to the CBR and BRN algorithms that reduces the node utilization. The utilization is sufficiently decreased such that higher values of w can be used to improve reliability while utilization is lower over all.

As discussed in our previous paper [18], the RCM employs Rayleigh fading to represent the cooperative nature of the BRN broadcasts. Thus, we anticipate that it is closer to the truly physical operation of a BRN. In figure 3, we show RCM results for what is otherwise the same set of CGM calculations used to generate the data for figure 2, including using the same ensemble of random networks. As can be seen, reliability is lower and utilization is higher.

This discrepancy is caused by cooperative broadcasting, which is represented in the RCM, but not in the CGM. Cooperative broadcasting increases the width of successive regions of RTS and CTS packets, and the corresponding SD and DS signals once the CBR has been formed. Referring back to figure 1, this corresponds to making the RTS/CTS annuli significantly thicker by node D/S than by S/D , which by itself can increase node utilization. In addition, under the original CBR formation algorithm, the only way to maintain

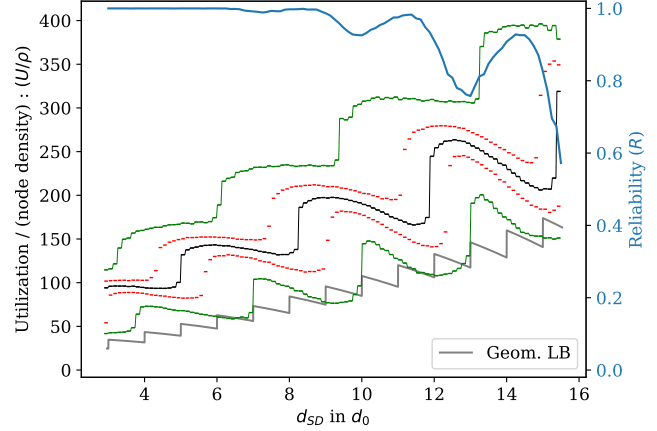


Fig. 3. Reliability and utilization results for discrete simulation of CBR formation using RCM. The set-up of this problem is identical to that shown in figure 2.

reliability is to increase w , further increasing required node utilization.

To compensate for this, we propose scaling the transmission power based on the local node density. In keeping with the goals of the BRN, this must be done without any information about the number or location of individual relay nodes. Our proposal includes the following modifications to the CBR formation algorithm, and the operation of the BRN:

- 1) Prior to each RTS/CTS packet, a pre-RTS/CTS packet (a *pre-packet*) is sent-out. All nodes transmitting the pre-packet simultaneously measure the incoming signal to approximate the number of neighbors broadcasting the same signal.
- 2) The transmission power for the actual RTS/CTS packet is then scaled at each node according to some formula, based on the received power of the pre-packet.
- 3) During unicast transmission, the nodes use this same scaling factor, the RTS scaling factor for the $S - D$ transmissions and the CTS scaling factor for the $D - S$ transmissions.

We recognize that this approach makes a few assumptions, which, we believe, must be addressed with a more detailed knowledge of hardware and the underlying dithering algorithm:

- 1) This assumes that the radios can operate in full duplex, accurately identifying and measuring the same received signal.
- 2) We are not aware if the dithering algorithm used by TrellisWare radios has been published, nor do we know if there is a limit to the number of simultaneous transmissions it can handle.
- 3) We assume within our simulation that the signal decays according to $d_{ij}^{-3.5}$. While this is reasonable for far-field communications, we have no controls within our simulations on the proximity of two randomly placed

nodes. Thus, in our simulations two nodes will often be placed much too closely for this formula to be physically reasonable, and will skew the scaling.

Despite these limitations, we employ a simple scaling formula, with no justification, other than that it appears to get the low- and high-density limits right:

$$P_s = P_f \max \left(p_b, \frac{1}{P_m/P_f + 1} \right), \quad (4)$$

where P_s is the scaled power for the RTS/CTS packet, P_f is the full power used in the pre-packets, P_m is the measured power, and p_b is an adjustable tuning parameter between zero and one. The tuning parameter ensures that P_s does not become too small when two nodes are very close. When p_b is 1, the algorithm is effectively the same as the unscaled RCM.

To assess the impact on the transmission scaling, we introduce three metrics, which are used to generate the plots in figure 4. For CBR calculations, we use the same calculation scenario, as described above, but also vary the node density. For $\rho = 15d_0$, we use the same random networks as before. We also employ a metric on the RTS formation, to investigate how the scaling affects this part of the geometry. For the RTS calculations, we use larger simulation domains, with side-length of $50d_0$, allowing us to consider more hops. For both the CBR and RTS calculations we use $p_b \in \{0.2, 0.5, 1.0\}$, where a value of 1.0 corresponds to unscaled transmission.

To assess how the transmission scaling impacts the RTS packets, we determine the center of each RTS shell by taking the expectation of the distance of the nodes i_{RTS} from the source, $E(d_{Si})$. We actually plot the difference between successive locations, recognizing that $d_{S0} = d_{SS} = 0d_0$. The results in figure 4 a. show that, provided p_b is tuned properly, it can cause the RTS/CTS annuli to have roughly uniform thickness even in the RCM. Otherwise, the annuli will grow with d_{Si} .

To measure reliability over a host of parameters, we note that in figure 3, there is oscillation with respect to d_{SD} . So, we choose a maximum distance, $15d_0$, and calculate the minimum expected value out to that distance, according to $\min_{d_{SD} \leq 15d_0} (R)$. These results, in figure 4 b., show that reliability is largely insensitive to p_b , provided ρ is sufficiently high. Though not shown here, we found in preliminary calculations that for all densities, a value of $p_b = 0$ is very unreliable. The most important factor for all of these is having a sufficiently high value of excess width, w .

Similar to the reliability, for utilization, we look at the expected value of the maximum utilization out to the given distance, $\max_{d_{SD} \leq 15d_0} E(U/\rho)$. Here, p_b has significant impact, while the impact of w is less than for reliability.

Taken together, the results presented in figure 4 suggest that transmission scaling can be used to reduce utilization without significantly affecting reliability, provided that the node density is sufficiently high. This is observed by comparing the distribution results in figure 3 with those given in figure 5. Using the transmission scaling here brings the curve near to the geometric LB for $w=3$, while the unscaled transmission

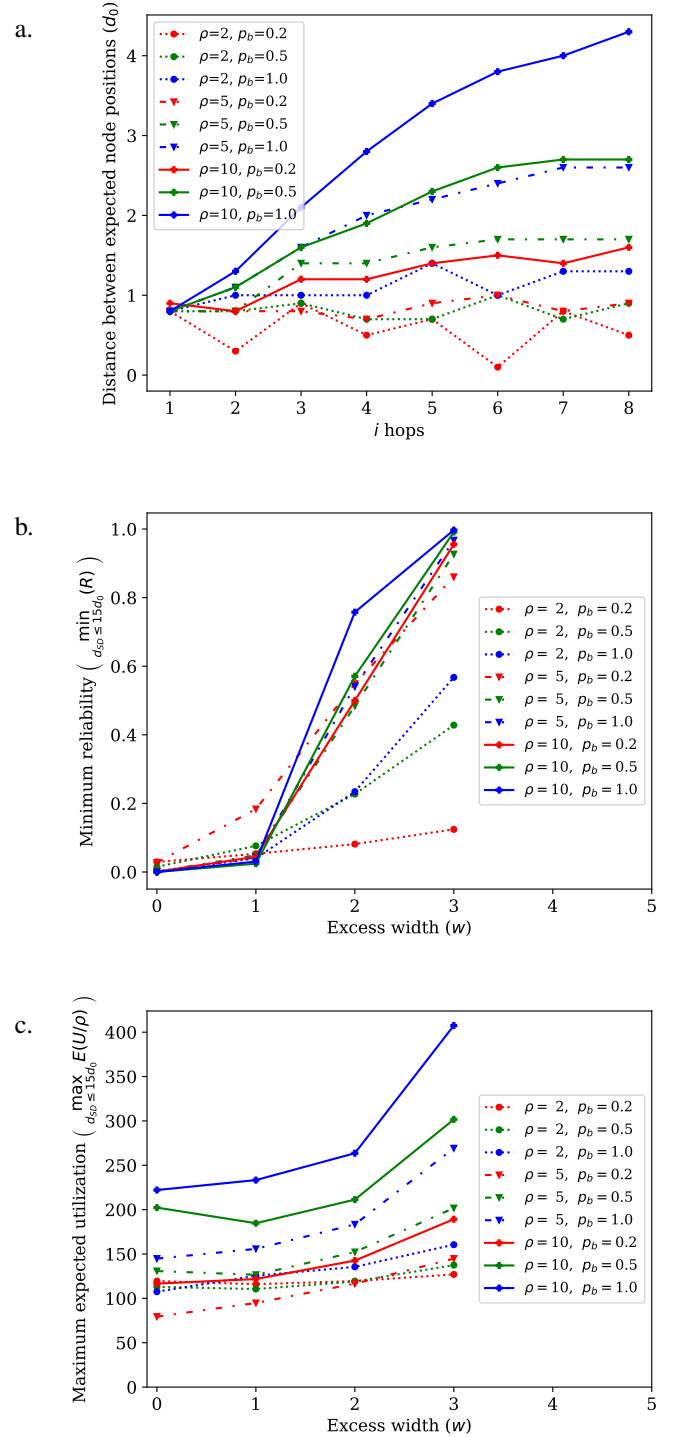


Fig. 4. Metrics to assess effects of transmission power scaling within RCM. a. As discussed in the text, this plot shows the differences between successive expected values for the distance of nodes i hops from S , $E(d_{Si})$. b. The computed minimum reliability for all simulations with $d_{SD} < 15d_0$, and varied values of ρ , p_b and w . c. The computed maximum utilization for all simulations with $d_{SD} < 15d_0$, and varied values of ρ , p_b and w .

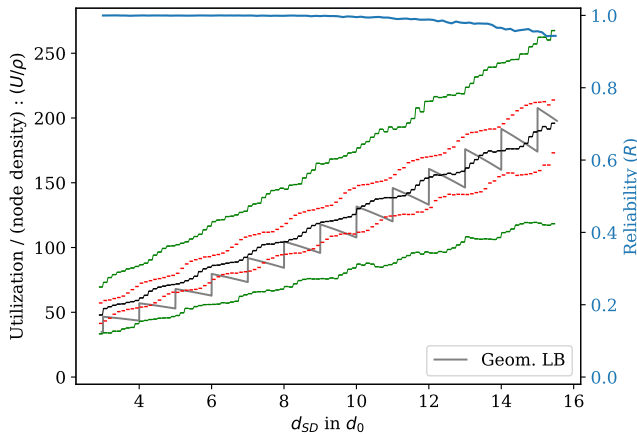


Fig. 5. Reliability and utilization results for discrete simulation of CBR formation using RCM and transmission scaling. The set-up of these simulations is identical to that shown in figure 3, other than the w was increased from 2 to 3, and transmission scaling has been used. Note that the Geom. LB increases with w .

is much more variable. We note, also, that provided the node density is sufficiently high, a $w > 2$ appears to be needed to ensure reliability.

One potential issue is that node density may be useful to determine the appropriate value for p_b . Here, however, some general information about the system may be inferred by the operator. For example, in many deployments, the operators may have a good general idea of the density of radios allowing rules of thumb to be developed for specific scenarios. However, it is also a single free parameter.

IV. CONCLUSION

In this paper, we have extended our earlier work on understanding how BRNs scale to higher node densities. While in our previous work we expressed concerns about higher densities, in this paper we find that transmission scaling can be used to decrease utilization to some degree, while ensuring reliability. We first analyzed CBR geometry within the CGM, showing that the CBRs are based on concentric circles and ellipses. We then discussed how the RCM modifies this geometry, and how this understanding could be used to modify CBR formation to decrease utilization while increasing reliability.

Modifications to BRN algorithms are significantly constrained by the design principle that no unique information about relay nodes can be added to the signal. Our proposed modification, adding pre-RTS/CTS packets to measure received signal during an RTS/CTS transmission, provides one possible means to extract some neighboring information within this constraint. Another possible method would be for each node to transmit short blips at random times within a pre-RTS/CTS time TDMA frame, to provide a means for a node to estimate the number of its neighbors.

We believe that the use of pre-RTS/CTS packets to derive a

transmission scaling, as described here, will translate to radio hardware, consistent with the specifics of the hardware and the dithering employed. The biggest questions revolve around how effectively a radio can estimate the number of neighbors. Thus, this may be as far as discrete event simulations can advance this line of research.

REFERENCES

- [1] A. Kott, A. Swami, and B. West, "The internet of battle things," *Computer*, vol. 49, pp. 70–75, 2016.
- [2] J. Burbank, P. Chimento, B. Haberman, and W. Kasch, "Key challenges of military tactical networking and the elusive promise of MANET technology," *IEEE Communications Magazine*, vol. Nov. 2006, pp. 39–45.
- [3] J. L. Burbank, P. F. Chimento, B. K. Haberman, and W. T. Kasch, "Key challenges of military tactical networking and the elusive promise of manet technology," *IEEE Communications Magazine*, vol. 44, no. 11, pp. 39–45, 2006.
- [4] K. Poularakis, G. Iosifidis, and L. Tassiulas, "Sdn-enabled tactical ad hoc networks: Extending programmable control to the edge," *IEEE Communications Magazine*, vol. 56, no. 7, pp. 132–138, 2018.
- [5] D. G. Reina, S. L. Toral, F. Barrero, N. Bessis, and E. Asimakopoulou, "Evaluation of ad hoc networks in disaster scenarios," in *2011 third international conference on intelligent networking and collaborative systems*. IEEE, 2011, pp. 759–764.
- [6] Y. Jin, X. Tan, W. Feng, J. Lv, A. Tuerxun, and K. Wang, "Manet for disaster relief based on ndn," in *2018 1st IEEE International Conference on Hot Information-Centric Networking (HotICN)*. IEEE, 2018, pp. 147–153.
- [7] I. Akyildiz, "A survey on sensor networks," *IEEE Communications Magazine*, vol. 40, no. 2, pp. 102–114, 2002.
- [8] M. Hammoudeh and R. Newman, "Adaptive routing in wireless sensor networks: QoS optimisation for enhanced application performance," *Information Fusion*, vol. 22, pp. 3–15, 2015.
- [9] M. Green, A. Thomas, A. Chachich, W. Fehr, and N. Towery, "FHWA white paper on mobile ad hoc networks," Tech. Rep. FHWA-HRT-18-027, US Department of Transportation, Federal Highway Administration, McLean, Virginia, 2018.
- [10] R. Ramanathan, "Challenges: A radically new architecture for next generation mobile ad hoc networks," in *Proceedings of the 11th annual international conference on Mobile computing and networking*. ACM, 2005, pp. 132–139.
- [11] T. Halford and K. Chugg, "Barrage relay networks," in *2010 Information Theory and Applications Workshop (ITA)*. IEEE, 2010, pp. 1–8.
- [12] "Information technology – Open Systems Interconnection – Basic Reference Model: The Basic Model," Standard, International Organization for Standardization, Geneva, CH, Nov. 1994.
- [13] T. Halford and K. Chugg, "The reliability multihop routes with autonomous cooperation," in *UCSD Inf. Theory and Appl. Workshop*, 2011.
- [14] T. Halford, K. Chugg, and A. Polydoros, "Barrage relay networks: System & protocol design," in *21st Annual IEEE International Symposium on Personal, Indoor and Mobile Radio Communications*. IEEE, 2010, pp. 1133–1138.
- [15] T. Halford, T. Courtade, and K. Turck, "The user capacity of barrage relay networks," in *MILCOM 2012-2012 IEEE Military Communications Conference*. IEEE, 2012, pp. 1–6.
- [16] S. Talarico, M. Valenti, and T. Halford, "Unicast barrage relay networks: Outage analysis and optimization," in *2014 IEEE Military Communications Conference*. IEEE, 2014, pp. 537–543.
- [17] S. Talarico, M. Valenti, and T. Halford, "Controlled barrage regions: Stochastic modeling, analysis, and optimization," in *MILCOM 2016-2016 IEEE Military Communications Conference*. IEEE, 2016, pp. 466–472.
- [18] N. Woolsey, Mingyue Ji, and B. Kraczek, "Predicting needs in future decentralized networks through analysis of barrage relay networks," in *2021 IEEE Wireless Communications and Networking Conference (WCNC)*, 2021, pp. 1–6.
- [19] Z. Wu, G. Menichetti, C. Rhamede, and G. Bianconi, "Emergent complex network geometry," *Scientific Reports*, vol. 5, pp. 10073, 2015.